ELSEVIER

Journal of Power Sources 97–98 (2001) 254–257

JOURNAL OF POWER SOURCES

www.elsevier.com/locate/jpowsour

A new class of materials for lithium-ion batteries: iron(III) borates

J.L.C. Rowsell, J. Gaubicher, L.F. Nazar*

Department of Chemistry, University of Waterloo, Waterloo, Ont., Canada N2L 3G1

Received 6 June 2000; received in revised form 30 November 2000; accepted 18 December 2000

Abstract

The first electrochemical investigation of transition metal borate structures are reported, focusing on $FeBO_3$ and Fe_3BO_6. In Fe_3BO_6, uptake of lithium initiates a two-phase process that results in framework disintegration, as expected from structural considerations and formation of an amorphous material that reversibly cycles lithium with a specific capacity of 450 mhA/g at an average potential of 1.6 V, in the regime of anode applications. Substitution of Fe(III) with other metals in the Fe_3BO_6 lattice is found to be detrimental to cycling behavior. Reduction of the particle size results in a reversible capacity up to 700 mAh/g, albeit with some fading on cycling.

1. Introduction

A recent trend in the search for new cathode materials has been the investigation of framework structures containing polyanions such as sulfates, phosphates, and arsenates. Structures based on 3-D lattices such as $LiFePO_4$ (olivine)-, $VOXO_4$- and NASICON-related frameworks built of $(XO_4)^{n-}$ tetrahedra and MO_6 octahedra have been explored as electrode materials [1–5]. These structures have been shown to be promising hosts for the reversible insertion of lithium, as the Li insertion potential can be ''tuned'' by varying X. Since the tetrahedral units raise the reduction potential of the adjoining metal by the inductive effect, applications have been in the cathode arena with specific hopes of developing a useful iron-based material. This oxide is both inexpensive and environmentally benign. Success has been found with the olivine $LiFePO_4$ which has been shown to achieve theoretical capacity at reasonably fast cycling rates, with an average potential of 3.4 V [2]. Structures containing boron polyoxoanions (borates) provide an attractive area of investigation, given the low atomic weight and high electronegativity of B (only somewhat less than P and As). In addition, boron can adopt a three- or four-fold co-ordination environment, affording greater variety in redox potential adjustment. To date, none of these structures have been explored.

Metal borates are simple to prepare, can be produced from inexpensive oxide starting materials, and display a variety of structures built from either trigonal planes, tetrahedra, or both. Common structures such as ludwigite, warwickite, and pinakiolite contain trigonal BO_3 units that link M(II) and M(III) octahedra, and are known for a myriad of metal combinations. Most pure-M(III) borates have the calcite structure (or aragonite, for the lanthanides), with the exception of $MnBO_3$ and Fe_3BO_6, the latter containing tetrahedral boron. We have begun our investigation with the Fe(III) borates, which are cheap and of negligible toxicity. We find that norbergite shows the best electrochemistry of this system, with good reversible specific capacity and fair recovery on cycling. The potential is too low for cathode applications but suited for anode applications. Ex situ XRD diffraction clearly shows that Li uptake is accompanied by structural decomposition. The effects of metal substitution and particle size reduction have also been investigated.

2. Experimental

Mixtures of $Fe_2O_3 + 4H_3BO_3$ were fired at 880°C for 2 days for the preparation of Fe_3BO_6. The synthesis of pure $FeBO_3$ required a more elaborate firing program: 2 days at 670°C followed by 1 day at 760°C, quenching in air, regrinding, and firing an additional 2 days at 860°C. Unreacted boron oxide was removed by washing with hot water, the filtered products were then dried at 150°C. Preparations were also made with α-Fe_2O_3 obtained from freeze-dried precursors [6], which results in the synthesis of Fe_3BO_6 at temperatures as low as 600°C, over 2 days with 10 equivalents of boric acid. Metal substitution in Fe_3BO_6

* Corresponding author. Tel.: +1-519-885-4637; fax: +1-519-746-0435.
E-mail address: lfnazar@uwaterloo.ca (L.F. Nazar).

0378-7753/01/$ – see front matter
PII: S0378-7753(01)00532-8

was achieved by grinding stoichiometric amounts of the necessary oxides or nitrates with the starting material and firing the pressed pellets. Substitution of 20% Al, 10% Cr(III), and 20% $Co(II)_{0.5}Ti(IV)_{0.5}$ was achieved by firing at 900–910°C for Al or Cr(III), and at 830°C for $Co(II)_{0.5}Ti(IV)_{0.5}$.

Electrochemical experiments were performed in Swagelok™ cells with metallic lithium as the anode. Battery mixtures were prepared with 70% active material, 24% carbon black to enhance conduction, and 6% polymer binder. Mixtures were cast on nickel discs as cyclopentanone slurries, and 1 M $LiPF_6$ in EC–DMC was used as the electrolyte. Galvanostatic cycling was performed at a cycling rate of 1 Li/10 h, corresponding to a current density of 10 mA/g. Potentiodynamic experiments were undertaken at a rate of 5 mV/10 h, and samples were equilibrated at the final voltage until the current reached 1 Li/1000 h.

3. Results and discussion

Two iron(III) borate phases can be prepared by solid state synthesis: $FeBO_3$ with the calcite structure, [7] and Fe_3BO_6 with the norbergite structure (Fig. 1a) [8]. The Fe_2O_3–B_2O_3 phase diagram predicts that the final product is only determined by the firing temperature in this excess boron oxide region [9]. $FeBO_3$ has a stability range of 680–800°C, while Fe_3BO_6 forms between 800 and 900°C, above which it melts incongruently. This greatly simplifies their syntheses as unreacted boron oxide is easily removed with water.

3.1. Structure

The calcite phase, Fig. 1a, is a well known structure which contains Fe^{3+} octahedra joined at the apices by trigonal borate groups. The norbergite structure (Fig. 1a) is related to that of olivine, in that both contain distorted hexagonal close-packing of oxygen. One can write the formula of norgbergite, Fe_3BO_6, as "$Fe_2B_{2/3}O_4$", from which it is clear by comparison to olivine (A_2BO_4) that there are 1/3 less tetrahedra per formula. This leads to a difference in cation ordering, and a 1.5-fold increase in the *b*-axis parameter. For the $LiM(II)PO_4$ olivines, the Li are accommodated in the row of octahedral sites indicated by the arrow in Fig. 1b. Extraction of Li from the structure leads to emptying of these sites followed by reinsertion in a relatively topotactic reaction. Both norbergite and olivine lack unoccupied octahedral sites that are not face-sharing with filled tetrahedra,

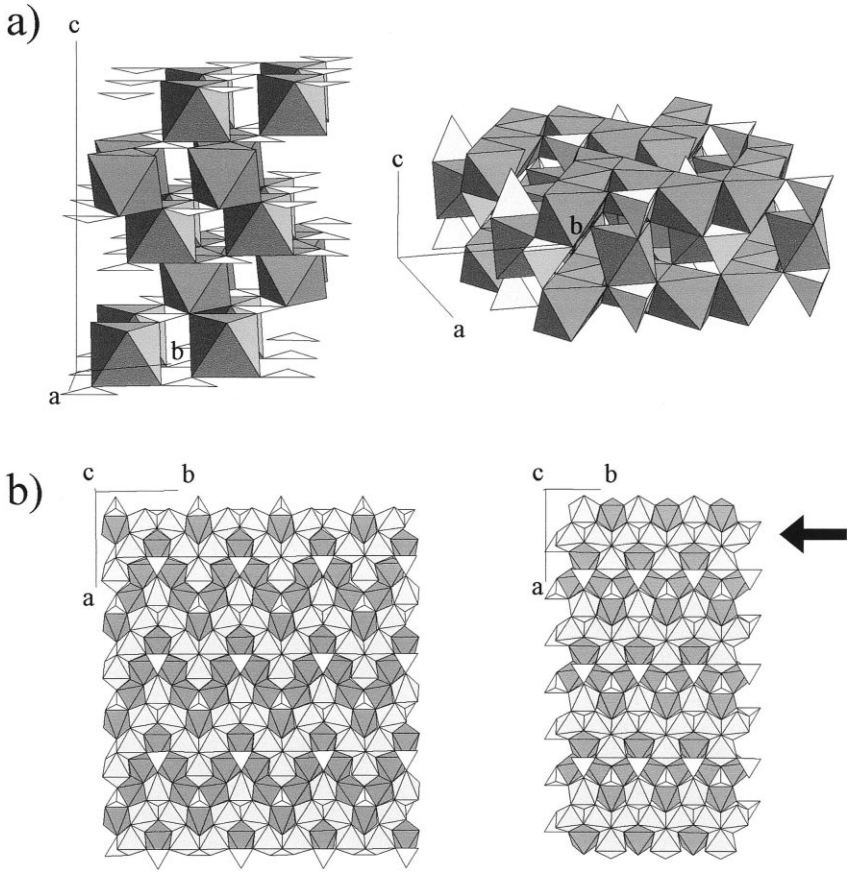

Fig. 1. (a) Polyhedral structures of $FeBO_3$ (left) space group R-3c: $a = 4.624$ Å, $c = 14.47$ Å; and Fe_3BO_6 (right) space group Pnma: $a = 10.048$ Å, $b = 8.531$ Å, $c = 4.466$ Å. The dark octahedra are Fe(III), light polyhedra are boron. (b) View along [0 0 1] of Fe_3BO_6 (left) and olivine (right). The lighter octahedra belong to the top layer. The row of octahedra indicated with the arrow contain Li^+ in $LiM(II)PO_4$ (see text).

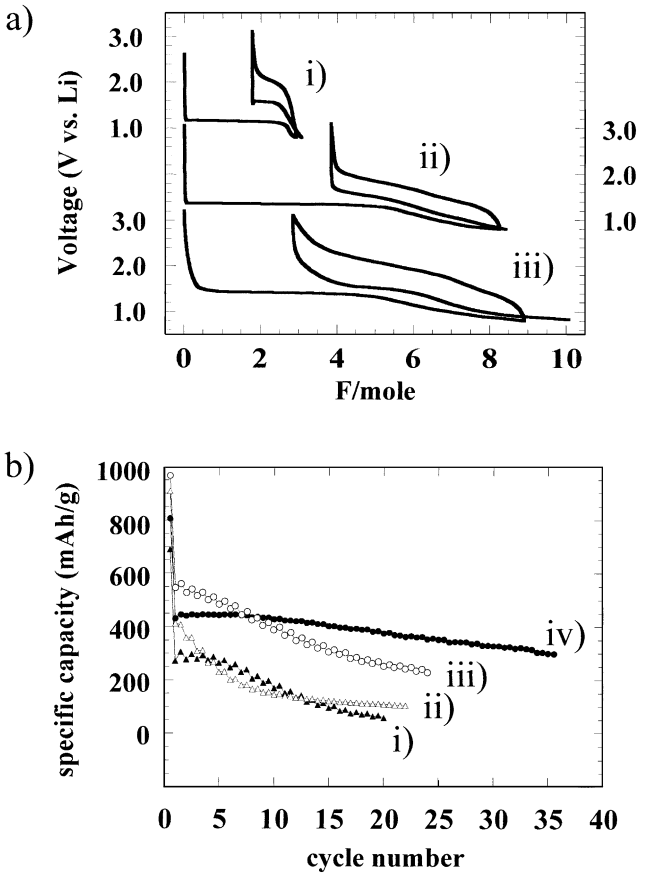

Fig. 2. (a) Discharge–charge curves for (i) $FeBO_3$; (ii) Fe_3BO_6 from the standard preparation at 880°C; (iii) Fe_3BO_6 synthesized at 700°C from lyophilized Fe_2O_3. A constant current density corresponding to the insertion of 1 Li/10 h in the potential window 0.8–3.1 V was used for each material. (b) Cycling performance of (i) $FeBO_3$ reduced to 0.8 V (▲); (ii) $FeBO_3$ reduced to 0.2 V (△); (iii) Fe_3BO_6 reduced to 0.2 V (○); (iv) Fe_3BO_6 reduced to 0.8 V (●). All materials oxidized to 3.1 V.

and both have only empty tetrahedral sites that are face-sharing with occupied octahedra. The insertion of lithium into Fe_3BO_6 is therefore expected to lead to decomposition of the framework, due to cationic repulsions.

3.2. Electrochemistry

The initial discharge–charge curves of both iron(III) borates are shown in Fig. 2a. Reduction in both compounds is marked by an abrupt decrease in voltage, indicating that no Li insertion occurs at high potential. This is followed by what appears to be a two-phase process. Nearly full theoretical capacity (from Fe^{3+} to Fe^0) is achieved in both materials upon reduction to 0.8 V. Somewhat more Li, however, is inserted upon further reduction to 0.2 V, to give an initial discharge capacity on the first sweep of 965 mAh/g ($x = 9.4$ Li after correction for carbon capacity) for the norbergite phase. As shown by the capacity recovery curves in Fig. 2b, Fe_3BO_6 shows the least amount of fading when the lower voltage cut-off is maintained at 0.8 V, but it is significant for

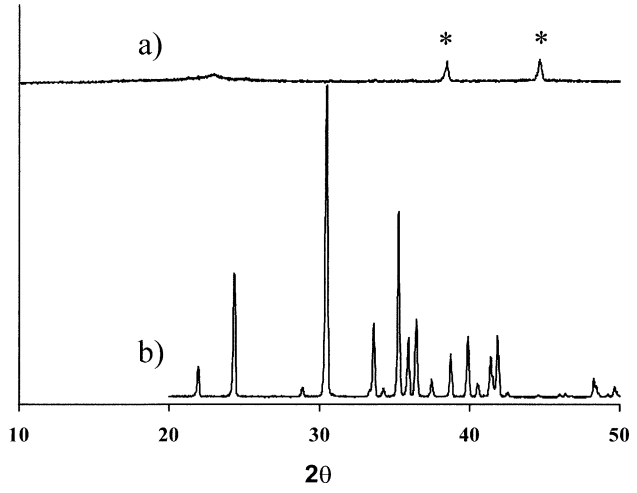

Fig. 3. Powder XRD patterns of (a) crystalline Fe_3BO_6; (b) the material after insertion of 5.2 Li (equilibration potential of 1.25 V). Asterisks indicate Al reflections from the sample holder.

the 0.2 V cut-off. Given the inferior behavior of $FeBO_3$, all consequent analysis was focused on the lithium uptake mechanism in Fe_3BO_6.

The nature of the first process is of particular interest. To examine this, a sample of Fe_3BO_6 was reduced to 1.25 V under potentiodynamic conditions. The chronoamperogram confirmed this was indeed a two-phase process with an equilibrium potential of 1.40 V. An ex situ XRD of the reduced sample revealed that the framework is decomposed into an amorphous material, as shown in Fig. 3. It is thought that the Fe(II) formed during Li uptake in simple oxides such as Fe_2O_3 disproportionates to form a series of lithium iron(III) oxide phases concurrent with the extrusion of metallic iron from the particles [11]. That material displays the expected reduction capacity ($3e^-/Fe^{3+}$) on discharge to low potential. Whether or not a similar mechanism is at work here, where BO_x forms an amorphous matrix separating very small particulates of Li–Fe–O phases, will be determined by Mössbauer and XAS experiments currently in progress.

3.3. Effect of substitution for iron(III)

Norbergite phases are not known to form for transition metals other than iron. In an effort to determine whether transition metal substitution on the Fe(III) site would affect the electrochemical behavior, the starting materials were reacted with stoichiometric amounts of Al, Cr(III), Co(II), and Ti(IV) oxides. By this method, substitution of 20% Al, 10% Cr(III), and 20% $Co(II)_{0.5}Ti(IV)_{0.5}$ into the norbergite lattice was achieved. Powder XRD measurements showed solid solution behavior, as the lattice parameters of Fe_3BO_6 changed linearly with mole fraction of substituent. The greatest change was in the *b*-parameter, which expanded ($Co(II)_{0.5}Ti(IV)_{0.5}$) or contracted (Al, Cr(III)). The extrapolated Al substituted lattice parameters agree with those of Al_3BO_6 [10]. Electrochemical Li insertion in these

metal-substituted samples showed that the equilibrium potential of the first two-phase process only varies ±0.05 V even at 20% substitution. The deflection is positive for lattice expansion, and negative for contraction. This is likely related to subtle changes in the M–O bond lengths on substitution. The theoretical capacity is also lowered according to the amount of substitution, and capacity recovery upon cycling is worse than in the pristine material. It can be concluded that the substituted metals are effectively inert electrochemically, and that the disorder that they impart on the lattice leads to faster fading, in a way that is not completely understood.

3.4. Effect of particle size reduction

Standard solid state preparation of Fe_3BO_6 yields particles ∼5 μm in size (as shown by SEM), however, the particle size can be reduced by modification of the synthesis procedure: this should enhance the redox kinetics of the phase decomposition process. By using nanoparticulate Fe_2O_3 (grain size ∼50 Å) as a precursor, we found that the norbergite phase is formed at temperatures as low as 600°C. Extensive line broadening occurs in the XRD pattern, as expected. The particle coherence length, as determined from analysis of the XRD lineshapes using the Scherrer equation was about 40 nm for materials treated at this temperature, and 70 nm for calcination at 700°C (5 h). SEM imaging revealed that the particles form agglomerates about 200 nm in diameter. Preliminary electrochemical studies on these materials show that a greater reversible capacity of 700 mAh/g can be obtained (Fig. 2a), but hysteresis is increased and the cyclability is not as good. How this behavior is related to structural decomposition is the topic of our current spectroscopic analyses.

4. Conclusions

The olivine-related norbergite phase, Fe_3BO_6, and calcite phase $FeBO_3$ uptake Li in their structure in a non-topotactic reaction that results in framework disintegration. The electrochemical properties of Fe_3BO_6 are better than the calcite phase, with respect to both capacity and stability. The former reversibly inserts Li^+ to yield a relatively stable capacity of 450 mAh/g, at an average potential of 1.6 V, placing this material in the anode arena of Li-ion battery electrodes. These properties are unfortunately still inferior to those of graphitic carbons in some respects. Future work will focus on determining the mechanism of Li^+ uptake/extraction by Mössbauer and XAS experiments, in addition to refining the synthetic conditions and particle size to enhance electrochemical performance.

Acknowledgements

We thankfully acknowledge Dr. E. Bermejo (Université de Paris VI) for supplying nanoparticulate Fe_2O_3 for our syntheses. LFN gratefully acknowledges funding from the NSERC strategic grants program and JR thanks NSERC for an Undergraduate Research Award.

References

[1] A.K. Padhi, K.S. Nanjundaswamy, J.B. Goodenough, J. Electrochem. Soc. 144 (1997) 1188.
[2] N. Ravet, M. Armand, in: Proceedings of the Abstracts of Electrochemical Society Meetings, Abstract #127, Honolulu, Vol. 99, no. 2, 1999.
[3] A.S. Andersson, J.O. Thomas, B. Kalska, L. Haggstrom, Electrochem. Solid State Lett. 3 (2000) 66.
[4] J. Gaubicher, F. Orsini, T. Le Mercier, S. Llorente, A. Villesuzanne, J. Angenault, M. Quarton, J. Solid State Chem. 150 (2000) 250.
[5] C. Masquelier, A.K. Padhi, K.S. Nanjundaswamy, J.B. Goodenough, J. Solid State Chem. 135 (1998) 228.
[6] E. Bermejo, T. Becue, C. Lacour, M. Quarton, Powder Technol. 94 (1997) 29.
[7] J.C. Joubert, T. Shirk, W.B. White, R. Roy, Mater. Res. Bull. 3 (1968) 671.
[8] R. Diehl, G. Brandt, Acta Cryst. B31 (1975) 1662.
[9] H. Makram, L. Touron, J. Loriers, J. Cryst. Growth 13/14 (1972) 585.
[10] J.J. Capponi, J. Chenavas, J.C. Joubert, Bull. Soc. Fr. Min. Cryst. 95 (1972) 412.
[11] M.M. Thackeray, W.I.F. David, J.B. Goodenough, J. Solid State Chem. 55 (1984) 280.